ORGANIC PROCESS RESEARCH & DEVELOPMENT
OPR&D
Article
pubs.acs.org/OPRD

Preparation of the HIV Attachment Inhibitor BMS-663068. Part 4. Synthesis of the 6-Azaindole Core

Michael S. Bultman,* Junying Fan, Dayne Fanfair, Michelle Soltani, James Simpson, Saravanababu Murugesan, Maxime Soumeillant, Ke Chen, Christina Risatti, Thomas E. La Cruz, Frederic G. Buono, Victor Hung, Richard L. Schild, Sabrina Ivy, Jason T. Sweeney, David A. Conlon, and Martin D. Eastgate

Chemical & Synthetic Development, Bristol-Myers Squibb Company, One Squibb Drive, New Brunswick, New Jersey, 08903-0191, United States

ABSTRACT: We report research focused on the construction of the 6-azaindole core, a key intermediate in the synthesis of the clinical candidate BMS-663068. The work describes an efficient and scalable method to access the 6-azaindole from a protected 3-ketopyrrole via a Pictet−Spengler cyclization and a radical-mediated aromatization. The process reported herein has been successfully implemented on the multikilogram scale to support preclinical development and clinical studies of BMS-663068.

INTRODUCTION

Key to the success of a commercial route to BMS-663068 (**1**) was defining a robust method to generate the 6-azaindole scaffold **5** (Scheme 1). Not only are there limited methods reported for the synthesis of 6-azaindoles, but those available were not amenable to large-scale applications with the desired substitution pattern.[1] We therefore invested significant efforts to devise an efficient and concise synthesis of the core **5** starting from pyrrole **6**.[2]

Herein, we describe the preparation of the 6-azaindole core **5** from ketopyrrole **2** by employing a Pictet−Spengler cyclization to access tetrahydroazaindole **4** followed by a radical-based aromatization (Scheme 1). The combination of these transformations proved uniquely effective for the synthesis of this bicyclic ring system. Vital to the success of the Pictet−Spengler cyclization was the use of a sp^3 hybridized substrate at the C4 position rather than sp^2 (likely due to both electronic and conformational advantages) requiring temporary protection of the ketone within **2**.

RESULTS AND DISCUSSION

Ketalization of **2** (Scheme 2) with ethylene glycol was achieved most efficiently in MeOH with sulfuric acid and trimethylorthoformate (TMOF).[3] The use of nonpolar aprotic solvents led to low conversions, even under azeotropic drying or strictly anhydrous conditions. We believe that MeOH serves multiple roles during this transformation by first facilitating deprotection of the *N*-formyl group to afford **7** and second via the formation of the corresponding dimethyl ketal (**8**).[4] This hydrolytically unstable intermediate then undergoes trans-ketalization with ethylene glycol to afford the more stable dioxolane **3**, which can be isolated and stored. In practice, **2** was first premixed with sulfuric acid in MeOH at 60 °C for 3−6 h, which effected partial deprotection of the *N*-sulfonamide formyl group to afford **7**. The reaction begins as a heterogeneous mixture and fully dissolves after ∼50% conversion of **2** to **7**. Achieving full dissolution prior to addition of the ketalization reagents (ethylene glycol and TMOF) was essential to obtain high quality product, as **3** crystallized directly throughout the ketalization and would entrap undissolved **2**. The low solubility of **3** in methanol resulted in a reactive crystallization that allowed for a facile direct isolation without the use of distillations or addition of antisolvents. This optimized process has been run reliably at 500 kg scale to produce **3** in ∼88% yield and with an average purity of 96.0 HPLC area %. The typical impurities observed in the product are unreacted **7** (2−5%) and **8** (<2.5%), which are well-tolerated in the following steps.

We then turned our attention to the Pictet−Spengler reaction. As previously discussed, this cyclization is only successful with the use of formaldehyde and the presence of the sp^3 center at the C4 position of the substrate **3**.[2] One important feature of this transformation is that the C4 ketal required for productive cyclization readily undergoes hydrolysis under the same reaction conditions generating the desired ketone **4** in a single step.

We conducted a comprehensive evaluation of the acid, solvent, and formaldehyde source to maximize the yield and purity of the cyclization product **4** (Scheme 3). Trifluoroacetic acid (TFA) in dichloromethane (DCM) provided the fastest and cleanest conversion of the acids[5] and solvents[6] explored. Solid paraformaldehyde (PFA) outperformed aqueous formalin and 1,3,5-trioxane as it yielded the cleanest reaction profile and is an inexpensive commodity material available on the metric ton scale. The initial process generated **4** in 75−85% yield and >99 HPLC area % purity after an aqueous workup to remove the trifluoroacetic acid and crystallization from a mixture of DCM, methyl tertiary butyl ether (MTBE), and isopropyl acetate (IPAc).

Special Issue: From Invention to Commercial Process Definition: The Story of the HIV Attachment Inhibitor BMS-663068

Received: April 23, 2017

DOI: 10.1021/acs.oprd.7b00152
Org. Process Res. Dev. XXXX, XXX, XXX−XXX

Scheme 1. Synthesis of 4-Methoxy-1-(phenylsulfonyl)-1*H*-pyrrolo[2,3-*c*]pyridine (5)

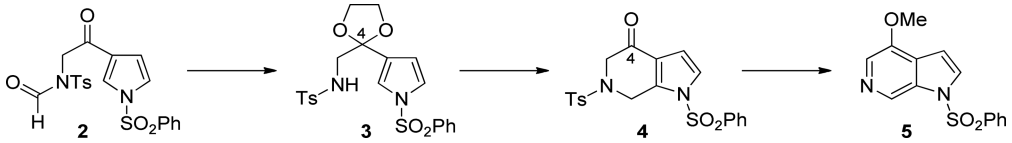

Scheme 2. Synthesis of Ketal 3

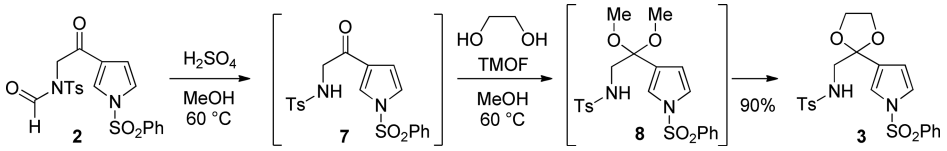

Scheme 3. Pictet–Spengler Cyclization To Generate 4

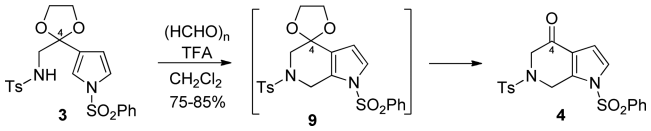

This procedure enabled initial material deliveries but presented a number of issues on larger scales (i.e., >5 kg). First, increased levels of multiple impurities were observed on scale resulting in lower isolated yields (65% vs 85%). Second, a TFA kicker charge was occasionally required to achieve full conversion. Finally, significant crusting of **4** on the reactor wall occurred during the crystallization leading to high product losses (8–15%).

To address these issues, we first turned our attention to the mechanism of the reaction as a starting point for our investigation of the yield and purity variability. The desired mechanistic pathway (Scheme 4, pathway A) generates the intermediate ketal **9**,[7] presumably via the *N*-sulfonyl iminium **10**.[8] Intermediate **9** could be observed by LCMS, but under the reaction conditions, it readily hydrolyzed to afford the desired ketone **4**. Alternatively, we envisioned an unproductive pathway could occur in which water, introduced in part from the PFA reagent, as well as generated by the reaction, would cause the hydrolysis of **3** to generate the ketone **7** (Scheme 4, pathway B). A series of control experiments showed that **7** does not undergo productive cyclization and is the source of the majority of the impurities observed at the end of the reaction. Thus, it was hypothesized that the yield loss correlates, to a large extent, with this initial undesired hydrolysis event. Therefore, we focused on reducing the extent of this undesired pathway as the first step to improving the reaction.

The rate of the desired transformation was affected by the low solubility of PFA in DCM as the reaction started out heterogeneous and turned homogeneous as it progressed. After evaluating different lots of PFA, we were able to establish a correlation between the rate of reaction, the physical properties of the PFA, and the yield of the reaction. A cursory analysis of the data suggested that better yielding reactions correlated with faster conversion of the input **3**, which occurred when PFA with a smaller particle size was utilized in the reaction (Table 1). However, an in-depth analysis of the physical properties of the batches of PFA showed that the true indicator for reaction performance was not simply the particle size.[9] We determined that the more significant difference in performance arose from the variation in the molecular weight of polymeric PFA.[10,11] NMR spectroscopy studies showed that no polymeric PFA was detected *in solution* for poorly performing lots of PFA. The limited solubility of the polymer, likely due to a higher degree of polymerization, reduces the presence of soluble formaldehyde-containing species during the initial stage of the reaction and therefore adversely affects the rate of the desired transformation.

An analysis of the kinetic profile was also consistent with this proposal, wherein a source of PFA with a low molecular weight (Table 1, entry 1) showed a rapid conversion of **3** to **4** and limited formation of the undesired hydrolysis product **7** (<0.5 HPLC area %) (Figure 1). Conversely, a source of PFA with a high molecular weight (Table 1, entry 3) showed a slower rate for the desired reaction and high levels of **7** (up to 6 HPLC area %). In both cases the concentration of **7** reached a

Scheme 4. Mechanistic Understanding of Pictet–Spengler Transformation

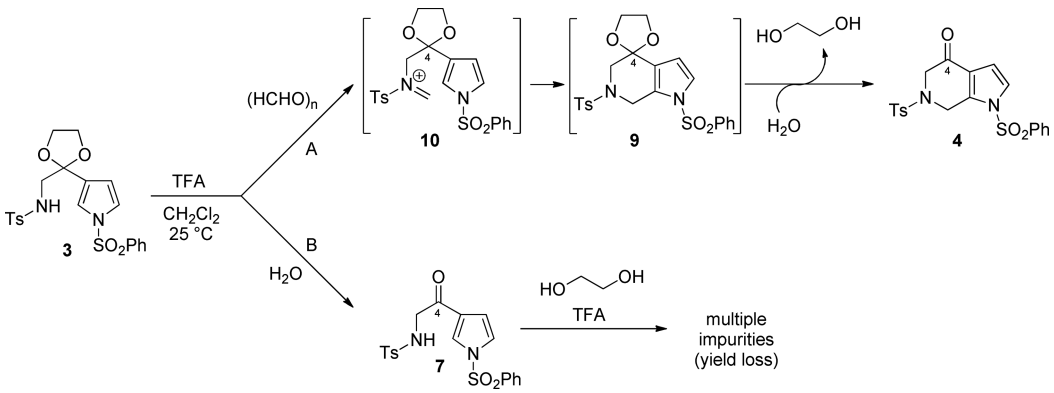

DOI: 10.1021/acs.oprd.7b00152
Org. Process Res. Dev. XXXX, XXX, XXX–XXX

Table 1. Effect of PFA Physical Properties during Pictet–Spengler Cyclization

entry	appearance	4[a]	rate[b]	particle size[9] (μm)	monomeric formaldehyde[c]	polymeric PFA[d]	polymer length n[e]
1	powdered	88.6	fast (<2 min)	90	yes	yes	10.6
2	granular	86.3	medium (10 min)	400	yes	yes	7.4
3	granular	83.0	slow (>30 min)	390	trace	no	NA

[a]Reactions conducted on a 1 g input. The particle size effect on the yield/purity was more pronounced on production scale. Reactions were analyzed by HPLC after 1 h, area % of **4**. [b]Time to achieve <2 HPLC area % of **3**. [c]Presence of monomeric formaldehyde observed in solution (^{1}H NMR in $CDCl_3$). [d]Presence of polymeric PFA observed in solution (^{1}H NMR in $CDCl_3$). [e]n = degree of polymerization ($HO(CH_2O)_nH$, ^{1}H NMR in $CDCl_3$) for polymer observed in solution.

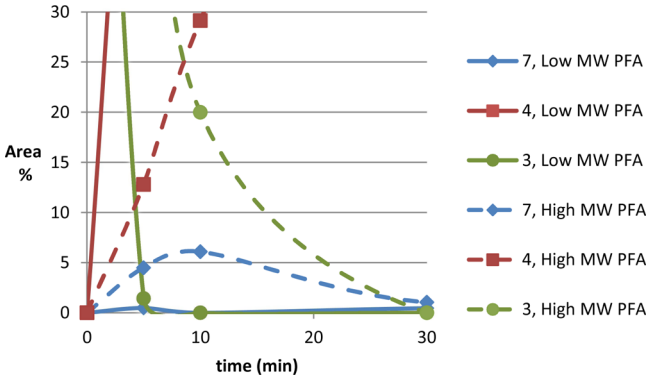

Figure 1. Kinetic profile of Pictet–Spengler cyclization with low and high MW PFA.

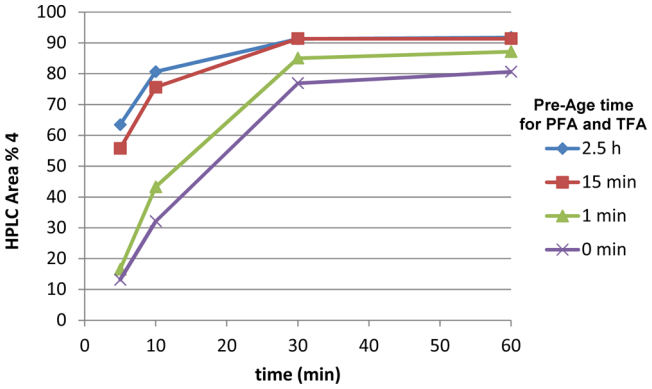

Figure 2. Effect on the reaction rate and yield of **4** by premixing high MW PFA with TFA.

maximum after 5–10 min and then decreased as it decomposed into a number of low level impurities via acid catalyzed processes. Collectively, the data support the hypothesis that the presence of high molecular weight PFA has a detrimental effect on the reaction performance due to reduced solubility.

With the cause of the reduced reaction yield identified, we focused on identifying a solution to this source of variability. The use of tight purchase specifications during the sourcing of PFA was deemed impractical and costly, and therefore, we focused on options for a reproducible reaction performance regardless of the polymer molecular weight. This was conveniently accomplished by altering the order of addition for the reaction. Premixing the PFA and the TFA led to a hazy or clear solution due to the reactive dissolution of the polymeric material.[12,13] This solution was then subjected to **3**, resulting in a scale-independent rapid transformation (<60 min) to form **4** in consistent yields with reduced levels of impurities and without the need for additional kicker charges of TFA. We established a minimum 2 h premixing age after studying the effect of premixing time for a high molecular weight batch of PFA on reaction performance (Figure 2). We were able to apply this simple procedural change to achieve comparable purity/impurity profiles and reaction rates regardless of the source or physical properties of the paraformaldehyde.[14]

We then studied the crystallization and isolation to prevent product crusting and its associated yield losses. DCM served as an ideal solvent for the reaction; however, the high solubility of product **4** in DCM required a labor and volume-intensive solvent exchange with MTBE/IPAc (10:1 v/v) to achieve acceptable yields at the crystallization end point. More importantly, a large amount of product (~15%) was lost to the reactor surface through crusting due to the large solubility swing during the solvent exchange. In an effort to simplify the isolation and reduce the amount of solvent utilized we developed and applied a solubility model (Figure 3)[15] which allowed for the maximization of the recovery of **4** while still maintaining acceptable solvent levels for production equipment. The application of these learnings resulted in the concentration of the DCM stream from 10 to 4 L/kg to achieve a relative supersaturation (C/C^*) of 120%, followed by seeding and slow addition of a single antisolvent (isopropanol, IPA), which allowed for isolation of the product with only 8% loss to the filtrate. This dramatically simplified the procedure, reduced the waste generation, and reduced losses from crusting to <1%. The process was further streamlined by running the Pictet–Spengler reaction at 4 L/kg DCM, without negative impact on yield or quality, thus eliminating the need for the postreaction distillation entirely. This optimized process has been reproducibly run at 480 kg scale to generate **4** in 81% yield and >99.0 HPLC area % purity.

With a streamlined and high-yielding process to generate **4**, we next focused on developing the aromatization process to access **5**. As previously described, this was the optimal strategy to install the C4 methyl ether in concert with oxidation of the six-membered ring.[2a] We had initially identified the use of methanesulfonic acid (MSA), TMOF, and cumene hydroperoxide (CHP) in MeOH as optimal conditions to effect the one-pot transformation involving ketalization of the C4 ketone, elimination to afford the methyl enol ether, and finally aromatization with the concomitant elimination of the sulfonate group (Scheme 5).

The transformation begins as a heterogeneous mixture of **4** in MeOH, which becomes homogeneous as a mixture of dimethyl ketal **11** and methyl enol ether **12** are formed.[16] Higher yields and quality of **5** were obtained when full dissolution was observed prior to the addition of the radical initiator. Initially, high temperatures were used (50–60 °C) to increase the rate of the reaction, but this depleted the TMOF via methylation of MSA.[17,18] Table 2 indicates that significant consumption of TMOF occurs in MeOH with MSA at 50 °C, independent of the water content. We therefore reduced the

DOI: 10.1021/acs.oprd.7b00152
Org. Process Res. Dev. XXXX, XXX, XXX–XXX

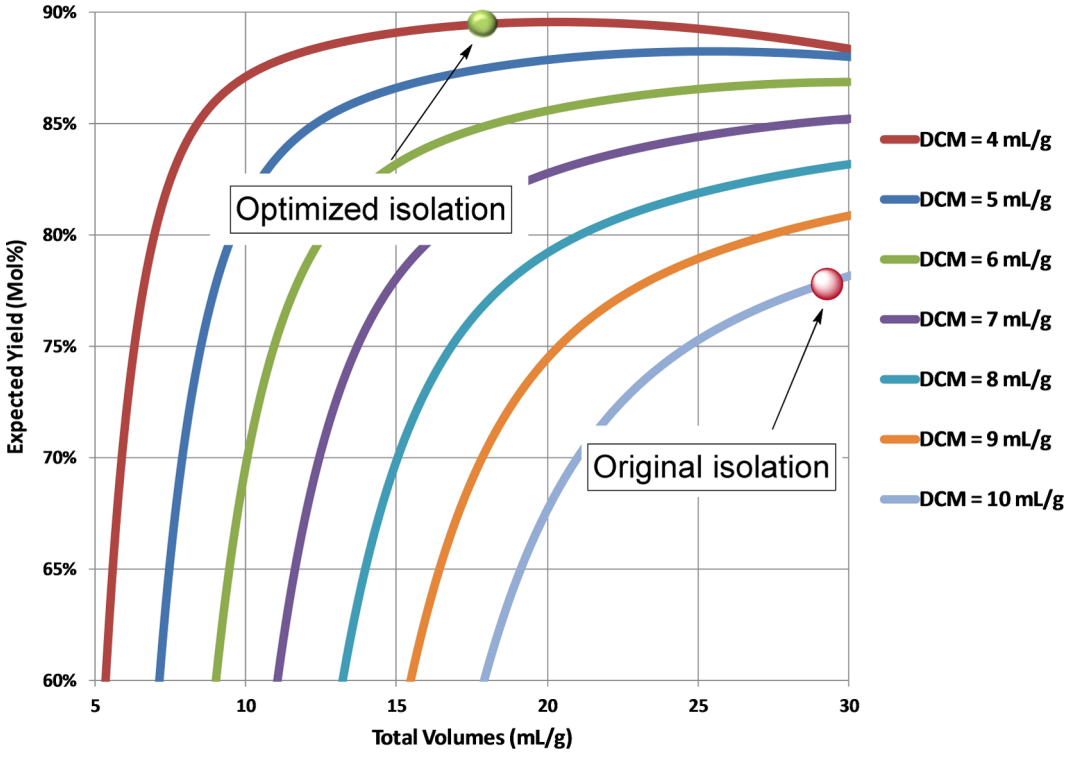

Figure 3. Solubility model for the yield optimization of **4**.

Scheme 5. Aromatization of Ketone 4

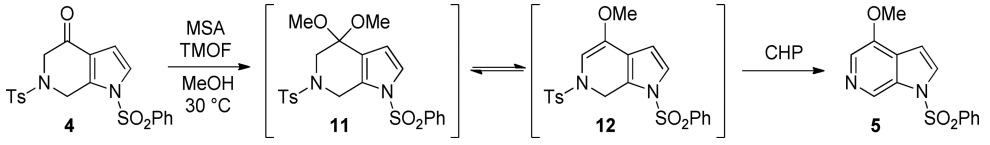

Table 2. Stability of TMOF in MeOH in the Presence of MSA

time (h)	temp. (°C)	H_2O (M)	TMOF remaining[a] (%)
2	50	1.0	15
2	50	<0.1	62
7	30	<0.1	92
24	20	<0.1	85

[a]Monitored by ^{1}H NMR and calibrated against an internal standard.

Table 3. Screening of Reaction Initiators for Conversion and Selectivity

entry	initiator/oxidant	SM conversion[a] (%)	over-oxidation byproducts[a] (area %)
1	<1% oxygen[b]	38	4
2	1% oxygen in N_2[c]	54	6
3	5% oxygen in N_2[d]	72	20
4	air	94	10
5	chloroanil[b,e]	90	15
6	benzoquinone[b,e]	65	20
7	potassium persulfate[b,e]	81	5
8	AIBN[b,f]	80	<0.5
9	TBHP[b,f]	90	<0.5
10	CHP[b,f]	95	<0.5

[a]Measured by HPLC analysis at 234 nm after 5 h. [b]Reactions run with N_2 atmosphere. [c]1% oxygen in N_2 was sparged through reaction solution. [d]5% oxygen in N_2 was sparged through the reaction solution. [e]Oxidant (1.0 equiv). [f]Initiator (0.4 equiv).

reaction temperature to 30 °C to balance reagent stability with reaction rate. DOE experiments demonstrated that a more consistent conversion was observed with >1.5 equiv of MSA and a relatively high charge of TMOF (5 equiv) provided desirable robustness to combat exogenous water and reduce the effect of the slow decomposition of TMOF during potential long reaction times.

The aromatization step is a radical-mediated process that can be induced by oxygen or other radical initiators.[2] Although the use of oxygen was efficient on the lab scale (Table 3, entry 4), its use for large-scale production posed concerns regarding safety and reproducibility, as well as the formation of difficult to purge overoxidation byproducts. We thus chose the readily available cumene hydroperoxide (CHP) as an optimal alternative (Table 3).

Under the selected reaction conditions (Table 3, entry 10), limited formation of **5** prior to the addition of CHP was observed (Figure 4). The addition of 0.1 equiv of CHP then led to the rapid formation of the desired product. Further experimentation showed variable conversion (<90 HPLC area % **5**) across a range of scales independent of the initial amount of CHP charged. We determined that the CHP was predominately consumed via a competitive reaction pathway originating from the known acid-mediated Hock rearrangement

DOI: 10.1021/acs.oprd.7b00152
Org. Process Res. Dev. XXXX, XXX, XXX−XXX

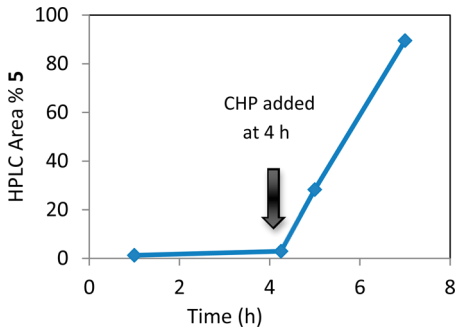

Figure 4. Kinetic profile for aromatization with delayed CHP charge. Reaction was carried out under N_2 atmosphere with MSA and TMOF. 0.1 equiv of CHP was added after 4 h.

to generate phenol and acetone.[19] The desired aromatization could be driven to full conversion by the addition of small kicker charges of CHP (0.25 equiv). The mechanism of this radical reaction is not fully understood; however, the working hypothesis suggests that the reaction is initiated via a minor decomposition pathway of CHP that involves C−O bond homolysis resulting in low concentrations of cumyl radical and/or peroxy radicals which then initiate the aromatization process.[20] The CHP protocol has been demonstrated on several 200−345 kg scale batches in which >99% conversion was consistently achieved.

We isolated azaindole **5** by first adding triethylamine to the MeOH solution to maintain a basic pH (>8) throughout the crystallization which minimized losses to the mother liquor. An aqueous solution of sodium thiosulfate was then added as antisolvent leading to the crystallization of the product and the reduction of any remaining CHP. The optimized process yielded **5** in 90−92% with excellent product quality and has been demonstrated in the preparation of over 2.4 MT of **5**.

CONCLUSION

We have developed a scalable synthesis of the 6-azaindole core for the preparation of **1**. The sequence entails a ketalization, a Pictet−Spengler cyclization, and an aromatization step. Key accomplishments include: (a) identification of robust conditions to achieve high conversion for a difficult ketalization substrate, (b) development of a reproducible procedure to utilize paraformaldehyde of variable molecular weight, and (c) identification of a robust radical-mediated aromatization process. We have applied a first-principles approach to improve each operation of the synthetic processes to the key 6-azaindole with improved yields and quality. Although the route includes the formation of seven intermediates, the sequence only involves three isolations, due to the judicious use of reagent combinations driven by mechanistic understanding and process controls.

EXPERIMENTAL SECTION

General. Reagents were used as received unless otherwise noted. Reported yields are for isolated materials or calculated solution yields and are corrected for potency. NMR spectra were recorded on a Bruker DRX-500 instrument and are referenced to residual undeuterated solvent. The following abbreviations are used to explain multiplicities: br = broad, s = singlet, d = doublet, t = triplet, q = quartet, m = multiplet. Infrared (IR) spectra were recorded on a PerkinElmer 1600 series FT-IR spectrometer. High-resolution mass spectra (HRMS) were recorded on a Thermo Orbi-trap Discovery instrument.

*Synthesis of 4-Methyl-N-((2-(1-(Phenylsulfonyl)-1H-pyrrol-3-yl)-1,3-dioxolan-2-yl)methyl)benzenesulfonamide (**3**).* To a 12 500 L reactor was charged methanol (9740 L, 20 L/kg), followed by the addition of solid **2** (487 kg, 1 equiv). Concentrated sulfuric acid (98 wt %, 11.1 kg, 0.1 equiv) was then added, and the mixture was heated up to 60 °C and aged for 3 h at which point a clear solution was achieved. Ethylene glycol (677 kg, 10 equiv) and trimethyl orthoformate (173 kg, 1.5 equiv) were then added, and the mixture was stirred at 60 °C for 6 h to achieve <3 combined area % of **2** and **7**. The mixture was cooled to 20 °C and aged at this temperature for 20 h to allow for complete desaturation. The resulting slurry was filtered, washed with MeOH (3890 L, 8 L/kg), and dried at 50 °C under vacuum to afford **3** (462 kg, 89.5%, 97.3 area %) as a white solid.

HPLC at 232 nm using Ascentis Express C18 2.7 μm 4.6 × 50 mm column, gradient method 40% B (0−4.5 min) to 100% B (6 min). Mobile phase A: 0.01% NH_4OAc in H_2O: MeOH (80:20), mobile phase B: 0.01% NH_4OAc in H_2O: MeOH: CH_3CN (5:20:75). Retention time: 3.0 min.

Melting point (mp) = 188−199 °C; ^{1}H NMR (500 MHz, $CDCl_3$) δ: 7.9 (d, J = 7.5 Hz, 2H), 7.7 (d, J = 7.8 Hz, 2H), 7.6 (t, J = 7.5 Hz, 1H), 7.5 (t, J = 7.5 Hz, 2H), 7.2 (s, br, 2H), 7.1 (s, 1H), 7.0 (s, 1H), 6.2 (s, 1H), 4.7 (s, br, 1H), 3.9 (s, br, 2H), 3.8 (s, br, 2H), 3.2 (d, J = 6.1 Hz, 2H), 2.4 (s, 3H). ^{13}C NMR (125 MHz, $CDCl_3$) δ: 143.30, 138.71, 137.31, 134.11 (2), 129.58 (2), 129.53 (2), 128.48, 127.00 (2), 126.91 (2), 118.67, 111.70, 105.47, 65.35 (2), 49.35, 21.53. HRMS [M + H; ESI$^-$] calcd for $C_{21}H_{23}N_2O_6S_2$: 463.0992; found: 463.0989.

*Synthesis of 1-(Phenylsulfonyl)-6-tosyl-6,7-dihydro-1H-pyrrolo[2,3-c]pyridin-4(5H)-one (**4**).* To a 8000 L reactor was added methylene chloride (1113 kg, 1.9 L/kg), followed by the addition of paraformaldehyde (88.5 kg, 3.1 equiv) and trifluoroacetic acid (379 kg, 3.5 equiv). The charge line was rinsed with dichloromethane (57 kg, 0.1 L/kg), and the mixture was stirred at 20 °C for 2−7 h to afford a clear solution. Methylene chloride (1170 kg, 2 L/kg) was charged to the reactor followed by the addition of **3** (440 kg, 1 equiv), and the mixture was aged at 20 °C for 1 h to achieve reaction completion. The reaction was quenched with 10% K_2HPO_4 aqueous solution (12 L/kg). The pH of the resulting aqueous phase is >3. The phases were separated, and isopropyl alcohol (1390 L, 4 L/kg) was added to the product-rich organic layer resulting in the formation of a product seed bed. The mixture was aged for 2 h, and then additional isopropyl alcohol (2780 kg, 8 L/kg) was added over 2 h. The slurry was cooled to 0 °C and aged for 2 h, at which point the solid was collected by filtration. The cake was washed with isopropyl alcohol (1390 kg, 4 L/kg) and dried at 50 °C under vacuum to afford **4** (336 kg, 81.3%, 99.5 area %) as a white solid.

HPLC at 230 nm using Phenomenex Kinetex, C18 100A, 4.6 × 150 mm column with gradient method 15% B (0 min) to 60% B (20 min) to 100% B (25 min) then 100% B (30 min). Mobile phase A: water (80%), methanol (20%) with 0.01 M NH_4OAc. Mobile phase B: acetonitrile (75%), methanol (15%), water (5%) with 0.01 M NH_4OAc, retention time: 20.33 min; melting point (mp) = 168 °C; ^{1}H NMR (500 MHz, $CDCl_3$) δ: 8.01 (dd, J = 8.4, 3.0 Hz, 2H), 7.78 (dt, J = 5.3, 1.2 Hz, 1H), 7.68 (t, J = 7.8 Hz, 2H), 7.30 (d, J = 8.4 Hz, 2H), 7.14 (d, J = 3.5 Hz, 1H), 7.07 (d, J = 8.1 Hz, 2H), 6.39 (d, J = 3.3 Hz, 1H), 4.85 (s, 2H), 3.95 (s, 2H) 2.33 (s, 3H); ^{13}C NMR

DOI: 10.1021/acs.oprd.7b00152
Org. Process Res. Dev. XXXX, XXX, XXX−XXX

(125 MHz, $CDCl_3$) δ: 187.0, 144.1, 137.9, 137.5, 35.3, 134.0, 130.2 (2), 129.8 (2), 127.4 (2), 127.1 (2), 122.7, 122.5, 108.3, 53.0, 43.2, 21.5; HRMS [M + H; ESI^-] calcd for $C_{20}H_{19}N_2O_5S_2$: 431.0730; found: 431.0722.

*Synthesis of 4-Methoxy-1-(phenylsulfonyl)-1H-pyrrolo[2,3-c]pyridine (**5**).* To a 8000 L reactor was charged methanol (4140 L, 12 L/kg), **4** (345 kg, 1 equiv), methanesulfonic acid (112 kg, 1.5 equiv), and trimethylorthoformate (413 kg, 5 equiv). The reactor was then inerted with N_2. The mixture was warmed up to 30−35 °C and aged for 2 h at which point cumene hydroperoxide (CHP, 90 wt %, 32.8 kg, 0.25 equiv) was added. After aging for 2−3 h another portion of CHP (32.8 kg, 0.25 equiv) was added and aged for an additional 2 h to reach reaction completion. After the desired conversion was achieved, the mixture was cooled to 20 °C and quenched with triethylamine (197 kg, 2.5 equiv) and then $Na_2S_2O_3$ (1 wt % aqueous solution, 4 L/kg). The mixture was allowed to age at 20 °C for 1 h to generate a seed bed. Additional $Na_2S_2O_3$ solution (1 wt % aqueous solution, 16 L/kg) was added slowly over 4 h, and the slurry was aged for 1 h and then filtered. The cake was washed with methanol/water (45/55, 10 L/kg) and dried until LOD < 0.5%. Compound **5** (207 kg, 91.4%, 99.6 area%) was obtained as an off-white solid.

HPLC at 230 nm using Phenomenex Kinetex, C18 100A, 4.6 × 150 mm column gradient method 15% B (0 min) to 60% B (20 min) to 75% B (25 min). Mobile phase A: water (80%), methanol (20%) with 0.01 M NH_4OAc. Mobile phase B: acetonitrile (75%), methanol (15%), water (5%) with 0.01 M NH_4OAc, retention time: 15.19 min; melting point (mp) = 152 °C; ^1H NMR (500 MHz, $CDCl_3$) δ: 9.01 (s, 1H), 8.03 (s, 1H), 7.92 (m, 2H), 7.68 (d, J = 3.9 Hz, 1H), 7.60 (dt, J = 7.8, 1.0 Hz, 1H), 7.49 (dt, J = 8.3, 1.9 Hz, 2H), 6.84 (d, J = 3.0 Hz, 1H), 4.00 (s, 3H); ^{13}C NMR (125 MHz, $CDCl_3$) δ: 149.6, 137.5, 134.5, 132.3, 129.6 (2), 129.1, 128.1, 127.6, 126.9 (2), 122.8, 105.6, 56.3; HRMS [M + H] calcd for $C_{14}H_{13}N_2O_3S$: 289.0641; found: 289.0639.

AUTHOR INFORMATION

Corresponding Author

*E-mail: michaelbultman@gmail.com.

ORCID

Michael S. Bultman: 0000-0002-0140-6120

Thomas E. La Cruz: 0000-0002-9745-4580

Martin D. Eastgate: 0000-0002-6487-3121

Notes

The authors declare no competing financial interest.

Michelle Soltani's maiden name is Michelle Mahoney.

ACKNOWLEDGMENTS

We thank the Chemical Development senior management for support during the preparation of the manuscript. The authors would also like to thank Alan Fritz, Dale Vanyo, and Simon Leung for chemical safety evaluation, Charles Pathirana for assistance with NMR, Mike Peddicord for assistance with mass spectroscopy, Victor Rosso for assistance with lab automation, and Francisco González-Bobes, Michael Schmidt, Richard Gaston, and Rodney L. Parsons for helpful discussions.

REFERENCES

(1) (a) Bartoli, G.; Palmieri, G.; Bosco, M.; Dalpozzo, R. *Tetrahedron Lett.* **1989**, *30*, 2129. (b) Bartoli, G.; Bosco, M.; Dalpozzo, R.; Palmieri, G.; Marcantoni, E. *J. Chem. Soc., Perkin Trans. 1* **1991**, 2757. (c) Blaazer, A. R.; Lange, J. H. M.; van der Neut, M. A. W.; Mulder, A.; den Boon, F. S.; Werkman, T. R.; Kruse, C. G.; Wadman, W. *Eur. J. Med. Chem.* **2011**, *46*, 5086. (d) Ganser, C.; Lauermann, E.; Maderer, A.; Stauder, T.; Kramb, J.-P.; Plutizki, S.; Kindler, T.; Moehler, M.; Dannhardt, G. *J. Med. Chem.* **2012**, *55*, 9531. (e) Huestis, M. P.; Fagnou, K. *Org. Lett.* **2009**, *11*, 1357. (f) Hands, D.; Bishop, B.; Cameron, M.; Edwards, J. S.; Cottrell, I. F.; Wright, S. H. B. *Synthesis* **1996**, *1996*, 877. (f1) Sakamoto, T.; Satoh, C.; Kondo, Y.; Yamanaka, H. *Heterocycles* **1992**, *34*, 2379. (h) Mahadevan, I.; Rasmussen, M. *J. Heterocycl. Chem.* **1992**, *29*, 359. (i) Whelligan, D. K.; Thomson, D. W.; Taylor, D.; Hoelder, S. *J. Org. Chem.* **2010**, *75*, 11.

(2) (a) Chen, K.; Risatti, C.; Bultman, M. S.; Soumeillant, M.; Simpson, J.; Zheng, B.; Fanfair, D.; Mahoney, M.; Mudryk, B.; Fox, R. J.; Hsaio, Y.; Murugesan, S.; Conlon, D. A.; Buono, F. G.; Eastgate, M. D. *J. Org. Chem.* **2014**, *79*, 8757−8767. (b) Eastgate, M. D.; Bultman, M. S.; Chen, K. C.; Fanfair, D. D.; Fox, R. J.; La Cruz, T. E.; Mudryk, B. M.; Risatti, C. A.; Simpson, J. H.; Soumeillant, M. C.; Tripp, J. C.; Xiao, Y. Methods for the Preparation of HIV Attachment Inhibitor Piperazine Prodrug Compound. U.S. Patent 2013/0203992, 2013.

(3) Conditions derived from Chan, T. H.; Brook, M. A.; Chaly, T. *Synthesis* **1983**, *1983*, 203 H_2SO_4 was chosen rather than HCl due to equipment compatibility..

(4) Observed by LCMS, when the reaction stream was quenched under basic conditions (DIPEA).

(5) Acids explored: triflic anhydride, sulfuric acid, boron trifluoride etherate, methane sulfonic acid, hydrochloric acid.

(6) Solvents explored: DCM, MeOH, DMSO, NMP, MTBE, AcOH.

(7) The hydrolytically labile reaction intermediates could be accurately monitored by HPLC if an organic base (e.g.; Hunig's base) was incorporated during the HPLC sample preparation.

(8) Pictet, A.; Spengler, T. *Ber. Dtsch. Chem. Ges.* **1911**, *44*, 2030.

(9) As measured for D(90) values acquired via MALVERN particle size analysis.

(10) As measured in solution via ^1H NMR in $CDCl_3$.

(11) Luftl, S.; Richaud, E. *Polyoxymethylene Handbook*; Luftl, S., Visakh, P. M., Chandran, S., Eds.; Scrivener Publishing: Salem, MA, 2014; pp 227−230, 277−280.

(12) Afforded mixture of smaller oligomers of paraformaldehyde as well as TFA bound species (^1H and ^{19}F NMR in $CDCl_3$).

(13) No detriment to quality or improvement to rate was observed if the TFA/PFA mixture was held longer the 2.5 h and less than 24 h.

(14) With this fundamental understanding of the reactivity of paraformaldehyde, it might be possible to develop the process in a greener solvent than DCM, however campaign timelines did not allow for further exploration.

(15) Solubility model for compound **4** as a function of IPAC concentration and initial CH_2Cl_2 quantity.

(16) As observed via HPLC and LCMS.

(17) Padmapriya, A. A.; Just, G.; Lewis, N. G. *Synth. Commun.* **1985**, *15*, 1057.

(18) The product of this undesired alkylation, methyl methanesulfonate, is also a known genotoxic impurity: Kazuhiko, T.; Chiharu, K.; Hiroaki, K. *Kankyo Hen'igen Kenkyu* **2000**, *22*, 163.

(19) Hock, H.; Lang, S. *Ber. Dtsch. Chem. Ges. B* **1944**, *77*, 257.

(20) (a) Ohkubo, K.; Yamabe, T.; Fukui, K. *Bull. Chem. Soc. Jpn.* **1970**, *43*, 1−8. (b) Timofeev, S. V.; Smirnova, A. L.; Blyumberg, E. A. *Kinetika I Kataliz* **1991**, *32*, 1225.

DOI: 10.1021/acs.oprd.7b00152
Org. Process Res. Dev. XXXX, XXX, XXX−XXX